IEEE Access
Multidisciplinary | Rapid Review | Open Access Journal

Date of publication xxxx 00, 0000, date of current version xxxx 00, 0000.

Digital Object Identifier 10.1109/ACCESS.2024.0429000

Analyzing the Efficacy of Computer-Aided Detection in Cerebral Aneurysm Diagnosis using MRI Modality: a Review

KEERTHI A. S. PILLAI[1], PREENA K. P.[2], and MADHU S. NAIR[3] , (Senior Member, IEEE)

[1]Artificial Intelligence & Computer Vision Lab, Department of Computer Science, Cochin University of Science and Technology, Kochi-682022, Kerala, India (e-mail: keerthias1988@gmail.com)

[2]Artificial Intelligence & Computer Vision Lab, Department of Computer Science, Cochin University of Science and Technology, Kochi-682022, Kerala, India (e-mail: preenakattel@gmail.com)

[3]Artificial Intelligence & Computer Vision Lab, Department of Computer Science, Cochin University of Science and Technology, Kochi-682022, Kerala, India (e-mail: madhu_s_nair2001@yahoo.com)

Corresponding author: Keerthi A. S. Pillai (e-mail: keerthias1988@gmail.com).

The author Keerthi A S Pillai is thankful to the University Grants Commission (UGC) of India for financial support through UGC-JRF fellowship- NTA Ref.No. 210510076010.
We also, acknowledge the support received from the computing facility at the Department of Computer Science, Cochin University of Science and Technology (CUSAT), sponsored by Kerala State Higher Education Council (KSHEC) under the Kairali Research Award 2020 Project (File No: KSHEC-A3/352/Kairali Research Award/47/2022).

ABSTRACT Computer-aided detection (CAD) models play a critical role in the clinical diagnosis of cerebral aneurysms, significantly contributing to the reduction of mortality rates associated with this condition. This article provides a comprehensive overview of the evolution of CAD models for aneurysm detection, with a particular focus on MRI modalities. It explores the motivations behind CAD systems, the methodologies employed, and their respective advantages and limitations, offering valuable insights into the current state-of-the-art (SOTA) CAD systems. The research papers selected for this review focus on research utilizing TOF MRA as the imaging modality and emphasize computer-aided detection through both traditional and deep learning techniques, with a particular emphasis on Convolutional Neural Networks (CNNs). CNNs have proven to be a crucial component in improving the accuracy and efficiency of aneurysm detection by automatically learning features from raw imaging data, bypassing the need for manual feature extraction. The article also presents a detailed experimental analysis of deep learning models, benchmarked using TOF MRA datasets. Key research gaps are identified, including the need for large training samples, challenges in Maximum Intensity Projection (MIP) imaging, limitations of 2D architectures, and issues related to overfitting and computational complexity. The review also observes that shallow networks and pretrained models are effective in addressing these challenges. In addition to identifying these gaps, the review outlines future directions for the development of CAD systems, aiming to further advance CAD models for aneurysm detection.

INDEX TERMS Cerebral Aneurysms, Computer Aided Detection, Magnetic Resonance Imaging, Machine Learning, Deep Learning, Convolutional Neural Networks.

I. INTRODUCTION

CEREBRAL aneurysm is a physical condition that causes weakness in the arterial walls of the brain with an increased risk of rupture [1]. A ruptured aneurysm is a prevalent condition for most non-traumatic subarachnoid hemorrhage (SAH), with a high mortality rate (23% - 51%) [2]. The International Study of Unruptured Intracranial Aneurysms (ISUIA) [3] informs that the rupture risk is closely associated with the size, shape, location, and morphological features of aneurysm and thereby closely monitoring these factors, clinicians can decide the treatment plan.

Health professionals use different imaging modalities [4] to analyse the morphological characteristics and location of the aneurysms. Unfortunately, because of its asymptomatic nature, clinicians often diagnose aneurysms in rupture situations or accidentally detect them from the images taken for other diagnostic purposes. Clinicians can address this situation by regularly monitoring the growth and rupture risk

of aneurysms in individuals with a family history or risk factors associated with aneurysms. Non-invasive magnetic resonance imaging (MRI) techniques [5], with time-of-flight magnetic resonance angiography (TOF MRA) in particular, have gained significant acceptance in monitoring tasks due to their non-invasive nature and ability to provide physiological parameters of vascular structures for accurately identifying and assessing the risk of aneurysm rupture.

A. WHAT MAKES CAD SYSTEMS NECESSARY?

Detection of cerebral aneurysms from TOF MRA volume is challenging for radiologists, especially for small-sized and medium-sized aneurysms, due to the overlapping of blood vessels in the maximum intensity projection (MIP) representation of TOF MRA volume. It may also lead to inter- and intra-observer variability in the diagnostic process. Hence, it is requisite to develop a computer-aided system to assist clinicians in their workflow by reducing the turn-around time, the chance of manual error, and under-detection. This impulse led to the development of computer-aided detection (CAD) systems in cerebral aneurysm detection.

This article provides a detailed review of the evolution of CAD systems in cerebral aneurysm detection using MRI modality. In general, CAD systems can be broadly classified into handcraft feature-based (first-generation) and deep learning-based (second-generation) systems. The reliability of the first-generation system is affected by the feature selection, while the second-generation systems learn features automatically from raw data and become more acceptable nowadays. However, deep learning is a data-driven approach demanding relevant and versatile samples for better performance.

B. RELATED SURVEYS

Few review articles [6]–[8] in the literature specifically address computer-aided cerebral aneurysm detection problems. Most focus on meta-studies and do not explore deeply into the computational approaches. Among the surveys, [6] discusses computational growth models used for rupture risk estimation rather than aneurysm detection and does not analyze performance using a common dataset. [7] is a meta-study that does not cover the theoretical aspects of computational approaches. [8] explores computational methods but lacks experimental evaluation. Additionally, the approaches differ based on the imaging modality, and there is a significant gap in the literature regarding reviews specifically focused on MRI-based aneurysm detection.

In this article, we aim to address these gaps by conducting an in-depth examination of various approaches utilized in existing CAD systems for cerebral aneurysm detection using MRI. We further provide a quantitative analysis of deep learning models, benchmarked against TOF MRA datasets, offering valuable insights into their performance and applicability.

C. KEY CONTRIBUTIONS OF THE ARTICLE

The major contributions of the article are:

1) The article provides a critical analysis of traditional methods, especially in handling 3D TOF MRA volumes for cerebral aneurysm detection, and discusses the need for deep learning-based approaches. Additionally, it emphasizes the importance of deep learning by demonstrating its superior ability to capture inherent patterns within 3D TOF MRA volumes.
2) Due to the unavailability of publicly accessible datasets for cerebral aneurysm detection from TOF MRA volumes, previous studies have not evaluated the efficacy of deep learning models under a common evaluation protocol. This article addresses this gap by conducting experiments on common datasets and comparing the performance of various deep learning models for aneurysm detection.
3) This article discusses the key observations from the experiments, emphasizing both theoretical and empirical limitations. This analysis helps researchers to identify the challenges faced by state-of-the-art models, particularly in the handling of 3D TOF MRA volumes for aneurysm detection.
4) The article provides a roadmap for future research, identifying critical gaps and discussing future directions for improving aneurysm detection from 3D TOF MRA volumes.

The remainder of this article is organized as follows: Section 2 provides a comprehensive overview of different approaches used in CAD systems; Section 3 discusses the observations from the experimental analysis of CAD systems with the TOF MRA challenge dataset; Sections 4 discuss the potential challenges and future perspective of CAD system development and section 5 summarize the contribution of this study.

II. EVOLUTION OF CAD SYSTEMS

Cerebral aneurysm detection using CAD systems can be considered as a three-stage process. The first stage is a pre-processing stage where the vascular regions are segmented for prioritizing candidates with a higher likelihood of aneurysm presence. In the second stage, candidate regions are chosen based on the extracted features or the training samples. In the final stage, false predictions are eliminated, and the confidence score of the developed model is improved. Fig. 1 briefly summarizes the pipelines of first and second-generation CAD systems.

A. FIRST GENERATION CAD SYSTEMS

First-generation (1G) CAD systems are semi-automatic because they build the model from handcrafted features, and the domain-specific pre-defined rules on these features decide the aneurysm candidate. The basic pipeline of a 1G CAD system consists of a pre-processing stage, candidate region identification, and false positive removal. Each stage is detailed in the following section, utilizing state-of-the-art methods available in the literature.

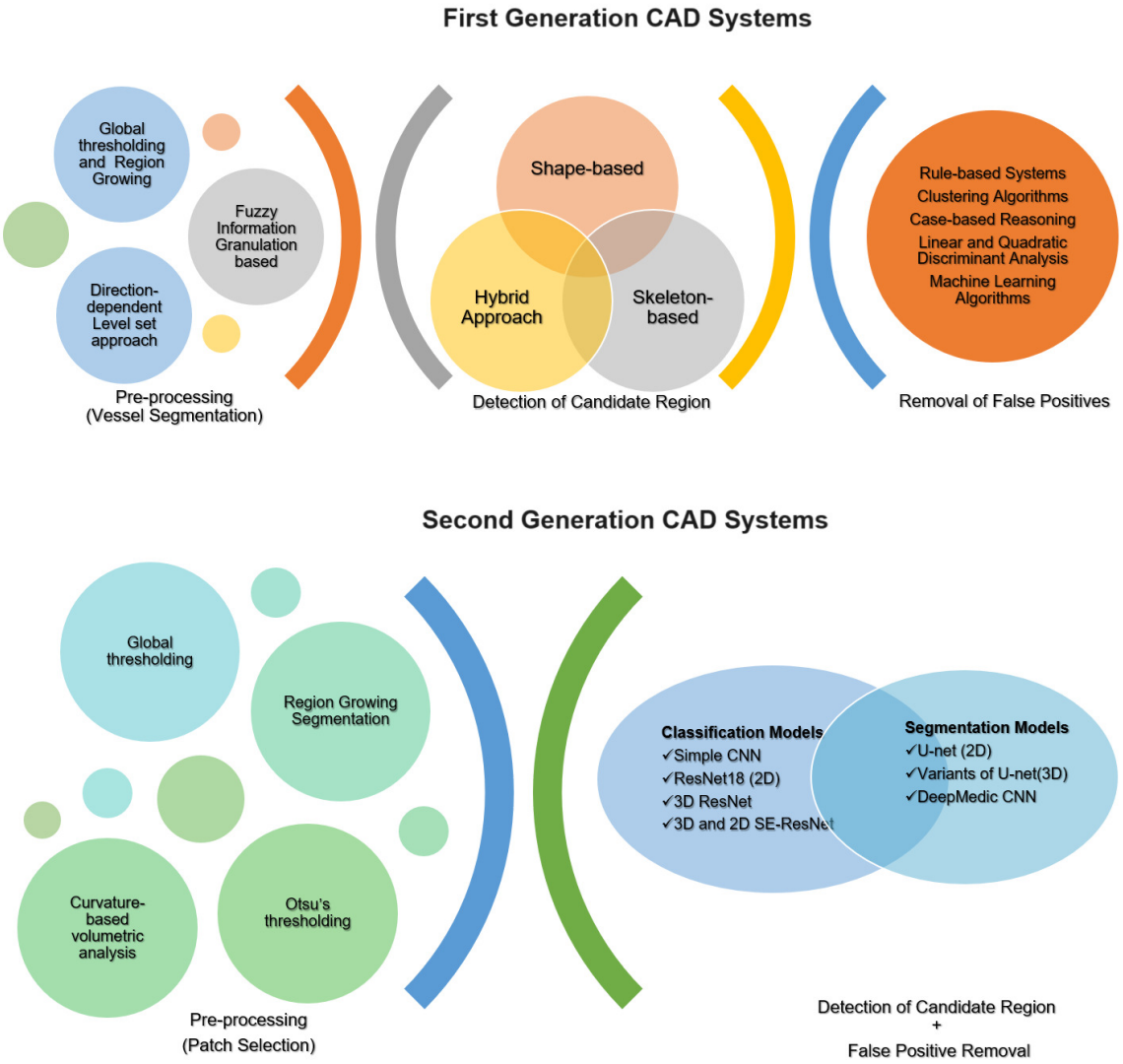

FIGURE 1. Comparison of pipelines used by 1G and 2G CAD Systems

1) Pre-processing Stage

In the pre-processing stage, 1G CAD systems adopt various vessel segmentation techniques for extracting the major vessel regions where the chance of aneurysm occurrence is very high. Arimura et al. [9] and Uchiyama et al. [10] in their works employed a global thresholding technique [11] to identify the vessel regions, with the threshold being determined by the linear discriminant analysis of the histogram. Kobashi et al. [12] applied a fuzzy information granulation (IG) methodology [13] to segment arterial vessels. This approach employs a fuzzy-model-based watershed segmentation to generate 3D quanta from the raw volume data, followed by a pre-trained neural network [14] that categorizes these units into vascular or background regions. Yang et al. [15] performed automated artery segmentation using a combination of global thresholding and region-growing segmentation techniques. Sunaiga et al. [16] employed a direction-dependent level set approach [17] for vessel segmentation. This approach utilizes the eigenvectors of vesselness filters [18] to incorporate direction information for direction-dependent level set vessel segmentation. Hanaoka et al. [19] extracted the vessel region by a conventional region growing method. In this method, a seed threshold $> \bar{I} + 3\sigma$ and a growing threshold $> \bar{I} + 2.5\sigma$ were applied, with $\bar{I}$ representing the average intensity and σ representing the standard deviation of the brain region. Nomura et al. [20] applied global thresholding followed by connected component analysis and morphological operations to extract vessel regions.

2) Candidate Region Identification

Following the identification of vessel regions, the first-generation CAD system proceeds to detect candidate aneurysm regions in the second stage with the help of filter-based approaches. The filter-based methods can be categorised into shape-based, skeleton-based, and hybrid depending on the information used to select candidate regions.

The shape-based methods [9], [10], [20]–[22] utilize filters designed to enhance the spherical or hemispherical shape, which is a characteristic feature of an aneurysm structure.

The methods in [9], [20], [22] incorporated eigenvalue analysis of the Hessian matrix in the filter design to enhance the aneurysm shape. Arimura et al. [9] use dot enhancement filters [23] that enhance dot-like structures by considering the magnitude and likelihood functions of these filters. The filter response is given as follows.

$$D(\lambda_1, \lambda_2, \lambda_3) = \frac{|\lambda_3|^2}{\lambda_1}, \qquad \text{if } \lambda_1, \lambda_2, \lambda_3 < 0 \tag{1}$$

where $\lambda_1, \lambda_2, \lambda_3$ represents the three eigen values of the Hessian matrix that satisfy $|\lambda_1| \geq |\lambda_2| \geq |\lambda_3|$. Then the aneurysm candidate is identified by using a gray-level thresholding technique on dot-enhanced images and region-growing method by monitoring some image features.

Nomura et al. [20] also use eigenvalue analysis of the Hessian matrix [18] to enhance blob, line, and bifurcation information, and the response is given by:

$$S_{blob}(\lambda_1, \lambda_2, \lambda_3) = \frac{|\lambda_3|}{\lambda_1}, \qquad \text{if } \lambda_1, \lambda_2, \lambda_3 < 0 \tag{2}$$

$$S_{line}(\lambda_1, \lambda_2, \lambda_3) = \frac{|\lambda_2| - |\lambda_3|}{\lambda_1}, \quad \text{if } \lambda_1, \lambda_2, \lambda_3 < 0 \tag{3}$$

$$S_{bifurcation}(\lambda_1, \lambda_2, \lambda_3) = S(\lambda_1, \lambda_2, \lambda_3) h(\lambda_1, \lambda_2, \lambda_3) \tag{4}$$

$$S(\lambda_1, \lambda_2, \lambda_3) = \frac{|\lambda_1 - \lambda_2| - |\lambda_2 - \lambda_3|}{|\lambda_1||\lambda_2|} \tag{5}$$

$$h(\lambda_1, \lambda_2, \lambda_3) = \exp(-\frac{\nabla I^2}{2\alpha^2}) \tag{6}$$

After computing these responses, they performed a voxel-based differentiation process [24] using the Mahalanobis distance ratio followed by morphological operation and connected component analysis to detect candidate regions.

Hentschke et al. [22] also use Hessian matrix-based blobness filters [25] that enhance blob-like structures to determine the initial candidate regions. The filter response is given by:

$$B(\lambda_1, \lambda_2, \lambda_3) = \frac{|\lambda_1|}{\sqrt{\lambda_2 \lambda_3}}, \quad \text{if } \lambda_1, \lambda_2, \lambda_3 < 0 \tag{7}$$

Then, a modified k-mean clustering is applied to this filtered image to decide the final volume of interest.

Uchiyama et al. [10] use a gradient concentrate (GC) filter [26] that effectively enhances and detects rounded convex regions of different sizes and contrasts. It is an iris filter that evaluates only the direction of gradient vectors without the magnitude. The filter can be represented as follows:

$$G(p) = \frac{1}{M} \sum_{R} \cos\theta_j \tag{8}$$

Here, M represents the total number of voxels where the gradient magnitude at position j is greater than zero, and θ_j represents the angle between the direction vector from point p to point j and a gradient vector at point j. The filter response is calculated within a sphere of radius R, centered at p. Subsequently, a gray-level thresholding is applied to the GC image to identify the aneurysm candidates.

The skeleton-based methods [12] utilize the vascular structure of arterial vessels to identify candidate regions. In vascular structure analysis, most approaches rely on thinning algorithms, which produce a skeletonized representation of arterial vessels.

Kobashi et al. [12] employ a 3D thinning algorithms [27] to generate thinning lines for segmented arterial vessels, estimate normal artery radii along these lines, and construct normal arteries. Candidate regions are then determined by subtracting these assumed normal arteries from the initially segmented arteries obtained in the pre-processing step.

The hybrid methods [15], [16], [19], [21] combine shape and skeleton based approaches to determine the candidate region.

Arimura et al. [21] use the shape-based difference image technique (SBDI) [28]–[30] and dot enhancement filtering in [23] to identify the various categories of candidate regions.

Yang et al. [15] employ a combination of a skeleton-based centerline computation method [31], a difference image technique [32], and dot enhancement filtering [23] to distinguish vessel, floater, and dot-type candidate regions from the extracted vascular structures. They use a 3D thinning algorithm [31] to identify vessel centerlines, which are transformed into trunk representations. The radius and length of each vessel segment at every trunk point are calculated using the inner tangent sphere testing method. Then the candidate regions are determined using distance transformation [32] and radius fitting techniques [15].

Suniaga et al. [16] apply an iterative thinning technique [31] to extract the 3D centerlines for identifying the endpoints and bifurcations in segmented vessels. Then, they utilize a vesselness filter [16], [18] based on the Hessian matrix to enhance blob-like features. Finally, they employ a 3D Forstner filter [33] to enhance structures with high surface curvatures.

Hanaoka et al. [19] introduced histogram of triangular paths in graph (HoTPiG), a novel graph-based representation for detecting abnormalities in vessel-like structures. HoTPiG captures morphological features and local branching patterns of graph nodes, and candidate regions are identified through a 3D histogram analysis of shortest-path distance-based nodes.

3) False Positive Removal

In the final stage of 1G CAD systems, features that support aneurysm detection are extracted, and mathematical or machine learning models are adopted for false positive removal. Table.1 provides the list of feature sets used in 1G CAD systems.

Arimura et al. in [9] and [21] use predefined rules on the extracted features followed by linear discriminant analysis (LDA) to filter out false positives. Similarly, Uchiyama et al.

TABLE 1. Feature sets used in 1G CAD systems

Model	Feature sets
Arimura et al. [9]	Average and standard deviation voxel value, effective diameter, sphericity, relative SD, maximum and minimum distance between centroid and surface, length of protrusion.
Uchiyama et al. [10]	Size, degree of sphericity, and mean value of GC image.
Kobashi et al. [12]	Spreadness, sphericity, intensity homogeneity and 3-D curvature.
Yang et al. [15]	Distance to the trunk, radius of the vessel, planeness, cylinder surfaceness, gaussian and mean curvatures, shape undex.
Sunaiga et al. [16]	Bifurcation distance, vessel thickness, blobness value, vesselness value, Forstner value.
Hanaoka et al. [19]	HoTPiG features and Hessian derived features (dot enhancement filters and shape index).
Nomura et al. [20]	Number of voxels and surface voxels, statistics of voxel values (minimum, maximum, mean, second moment, standard deviation, skewness, kurtosis and entropy), contrast measures, sphericity, similarity of sphere, statistics of the distance between the center of the candidate and its boundary, statistics of shape index and curvedness.
Arimura et al. [21]	Average and standard deviation voxel value, effective diameter, sphericity, relative SD, maximum and minimum distance between centroid and surface, length of protrusion and maximum or average distance value of distance-transformed image.
Hentschke et al. [22]	Average, minimum and maximum values of intensity, blobness and vesselness, distance of the region of interest(ROI) to the image boundary.

[10] use a rule-based system to eliminate false alarms and perform a quadratic discriminant analysis (QDA) to further reduce false positives (FP). Kobashi et al. [12] implement a case-based reasoning system [34] based on fuzzy logic to assign confidence scores to detected candidate regions, effectively eliminating false positives.

Hentschke et al. [22] performed feature analysis with the help of rule-based systems and removed false positives by assessing the symmetric similarity measure of features. Yang et al. [15] developed a rule-based system that eliminates most false positives while assigning probabilities to the remaining candidates. Subsequently, clustering algorithms select candidates with the highest likelihood from each cluster.

Recently, rule-based systems in 1G CAD systems have been replaced with machine learning algorithms, and [16] and [19] use support vector machine [35] for feature analysis and effectively categorize true positives and false positives.

Nomura et al. [20] studied how re-training a classifier affects 1G CAD system performance in a clinical setting. They used an ensemble classifier [36] and found that CAD system performance is closely related to the quality and quantity of extracted features. Miki et al. [37] analyzed radiologist's performance in a clinical environment with the model in [20] and found that the CAD system's assistance enhances the clinical workflow.

Table. 2 gives an overview of the first-generation CAD systems in the literature. From the literature, it is clear that CAD system performance highly relies upon features' quantitative and qualitative properties, and feature engineering plays an essential role in model development. It necessitates an automated tool that inherently extracts suitable features from the data and serves the CAD system's objective.

B. SECOND GENERATION CAD SYSTEMS

Second-generation (2G) CAD systems employ deep learning [38], particularly convolutional neural networks (CNNs), to automatically learn relevant features and perform complex data analysis through convolution process. In 2G CAD systems, the CNN model performs the feature engineering and feature analysis tasks to identify aneurysm candidates with fewer false positives.

2G CAD systems can be classified into classification and segmentation models based on their task. The classification model categorizes MRI slices as either benign or malignant, leading to a quicker turnaround time for routine analysis as clinicians focus exclusively on the malignant data. The segmentation model assists clinicians in categorizing aneurysm cases into different risk categories and determining the proper

TABLE 2. Summary of first-generation CAD Systems

Model	Pre-processing	Candidate Region Detection	FP Removal	Disadvantages
Arimura et al. [9]	Global thresholding	Dot enhancement filter with region growing (Short and Large type), local structures based on skeleton image (Short branch, single vessel and bifurcation type).	Rule-based system with LDA	Specificity of the model would depend on the patient with other vascular diseases. Under detection of large and short-branch type small aneurysms.
Uchiyama et al. [10]	Global thresholding	Gradient concentrate filter with thresholding	Rule-based system with QDA	Only small type aneurysm was considered for study. Difficult to quantify the shape using the sphericity feature alone which will lead to more FP.
Kobashi et al. [12]	Fuzzy information granulation(IG) based segmentation with pretrained neural network	Normal artery model using Thinning algorithms	Case-based reasoning	Under detection of aneurysms in the straight artery. Fusiform aneurysms are not considered for study. Features used are redundant which lead to more FP.
Yang et al. [15]	Region growing segmentation with thresholding	Hybrid approach which uses thinning algorithms for vessel POIs, difference image based technique with region growing for floater POIs and dot-enhancement filter for dot POIs.	Rule-based system with clustering	Low sensitivity to aneurysms nearby, as well as for recurrence or residual aneurysms.
Sunaiga et al. [16]	Direction dependent level set method	Hybrid approach that uses iterative thinning alogithms for endpoints and bifurcation, blobness filter for blob like structures and Forstner filter for structures with high surface curvatures.	SVM	Choice of kernel function has a crucial impact to the classification. Only saccular aneurysm have been used in the study.
Hanaoka et al. [19]	Region growing method with thresholding	Histogram of Triangular Paths in Graph (HoTPiG) Feature Set	SVM	Evaluate only shape of the tissue and discard all image intensity information. Under detection of small aneurysms.
Nomura et al. [20]	Global thresholding with connected component analysis and morphological operations	Eigenvalue analysis of Hessian matrix with a voxel based differentiation process based on Mahalanobis distance	Ensemble of weak classifiers	Candidate region identification using voxel based differentiation was computationally complex.
Arimura et al. [21]	Global thresholding.	Dot enhancement filter with region growing (Short and Large type), local structures based on skeleton image (Short branch, single vessel and bifurcation type), Shape-based difference image (SBDI) technique (single vessel and bifurcation type).	Rule based system with LDA	Under detection of large and short-branch type small aneurysms.
Hentschke et al. [22]	-	Blobness filter with K-means clustering	Rule-based system with symmetric similarity measure	Sensitivity and feature selection depends on the modality. Under detection of small aneurysms.

treatment plan by giving a semantic segmentation of the given TOF MRA volume. The following sections provide an in-depth look at the existing methods employed for classification and segmentation in the context of aneurysm detection.

1) Classification Models

This section outlines the various CNN models used for aneurysm classification in the literature. Since the performance of CNN networks is highly influenced by data distribution, the selection of training samples plays a vital role in the performance of the trained model. Therefore, the classification models have employed artery vessel segmentation techniques as a pre-processing step.

Nakao et al. [39] use the segmentation method in [19] for extracting arterial vessel patches for training. Ueda et al. [40] employed a curvature feature-based volumetric analysis [41] to identify the patches with abnormalities like true aneurysms, infundibular dilations, vessel bifurcations, and vessel stenosis. These patches are then used for training the model. Terasaki et al. [42] use a global thresholding technique

to segment vessel patches. Joo et al. [43] employ a two-stage vessel segmentation approach [44]. The first stage involves segmenting foreground and background regions using Otsu's method, while the second phase utilizes statistical distribution-based thresholding to extract vessel regions from foreground pixels.

Various augmentation techniques are employed in 2G CAD systems to generate sufficient positive samples to meet the requirement of balanced data distribution for classification models. Also, downsampling is applied to balance negative samples with positive ones. The downsampling process involves either random selection or a gradient decision tree-based classifier. In the second stage, raw patches from the segmented artery regions are fed into the convolution layer of DNN for feature extraction. The obtained feature maps with suitable activation function decides the probability of aneurysm occurrence.

Classification models in the literature use variants of CNN [38] for inherent feature engineering and decision-making. Nakao et al. [39] presented a 2D CNN-based model employing MIP representation of arterial voxel patches for aneurysm prediction. Similarly, Ueda et al. [40] utilized MIP of various arterial patches (arterial abnormalities, aneurysms, and bifurcation) to train a 2D ResNet18 [45] model. However, relying on MIP and 2D architecture might compromise topological information, potentially resulting in increased false alarms in these approaches [39], [40].

Joo et al. [43] employ a 3D ResNet-based architecture [46] for aneurysm detection, utilizing the topological information from the 3D arterial voxel patches. Terasaki et al. [42] incorporate topological and spatial information in their model using a multipath architecture of SE-ResNet [47] with a 3D network path for raw TOF MRA volume and a 2D network path for MIP of arterial patches. However, these models [42], [43] demand large training samples to avoid overfitting and are also computationally complex due to the number of parameters associated with the 3D model.

2) Segmentation Models

U-net [48] variants are widely employed in the segmentation task for accurate aneurysm localization. These models learn the inherent features suitable for pixel-wise classification (semantic segmentation) from the raw TOF MRA patches, and hence eliminating inter-observer variability in aneurysm size estimation.

Stember et al. [49] introduced a model for aneurysm segmentation based on the 2D U-Net architecture with MIP patches. The use of this 2D-based architecture adversely impacts the sensitivity of aneurysm detection due to the limitations of the 2D representation.

To overcome the drawback of 2D representation, Schitermann et al. [50] presented a model that uses DeepMedic architecture [51], a multi-scale, multi-path 3D CNN for semantic segmentation of TOF MRA volume. The size estimation of segmented aneurysms is quantified by employing a conditional random field (CRF) [52] in the pipeline. Since each input TOF MRA patch contains normal and aneurysm tissue, the model alarms many false positives, which is undesirable for the CAD system.

To reduce the false positives, Claux et al. [53] use bi-sequence 3D network architecture in which the first network employs an artery segmentation, and the latter performs the localization task. The segmentation network uses a modified version of U-net architecture and utilizes the topological information from the binary mask produced by the first network for segmenting the aneurysm.

Dataset annotation for model development is time-consuming, requiring experienced radiologists to generate binary masks or labels for specific data distributions. This results in insufficient training samples for creating models in the aneurysm detection domain. Di Noto et al. [54] addressed this issue by proposing a weak label scheme for training the model. This method uses a customized 3D U-net architecture [55] and employs anatomically informed sliding window approaches for selecting positive and negative samples.

Table. 3 summarizes 2G CAD systems in the literature. However, the performance of the 2G CAD systems are highly affected by the availability of training patches needed to optimize the trainable parameters of the model.

III. EXPERIMENTAL ANALYSIS OF STATE-OF-THE-ART CAD SYSTEMS

This section provides an insight into the factors that affect the 2G CAD systems performance by analyzing the classification models in the literature with the publicly available LAUSANNE Dataset and Aneurysm Detection and Segmentation (ADAM) [56] challenge dataset. This was the first article that experimentally analysing the CAD systems with standard datasets and provided observations that help in the CAD system development.

A. DATASETS

This section provides a demographic analysis of the datasets used in this study. A significant challenge in aneurysm detection research is the limited availability of publicly accessible datasets, as most related works rely on in-house datasets that are not publicly available. For our experimental analysis, we utilized the ADAM and LAUSANNE datasets, as they are the only datasets available for our study on cerebral aneurysm detection. While the LAUSANNE dataset is publicly available, access to the ADAM dataset requires official registration for the MICCAI 2020 ADAM Challenge.

1) ADAM Dataset

The ADAM dataset is adopted from the Aneurysm Detection And segMentation (ADAM) Challenge 2020 [56] conducted in connection with the Medical Image Computing and Computer Assisted Intervention Society Conference (MICCAI 2020). The training set of ADAM challenge consists of 113 cases, with 93 aneurysm cases and 20 normal scans. One-quarter of the scans have more than one aneurysm, and a total of 125 saccular type aneurysms are present in

TABLE 3. Summary of second-generation CAD Systems

Model	Pre-processing	Model Type	Deep Learning Model	Input Type	Loss Function	Disadvantages
Nakao et al. [39]	Region growing method with thresholding	Classification	4-layer CNN	2D MIP vessel patches	Binary cross entropy	Under detection of small aneurysm in the overlapped region due to MIP representation.
Ueda et al. [40]	Curvature feature-based volumetric analysis	Classification	ResNet18	2D MIP abnormal vessel patches	Binary cross entropy	Under detection of large aneurysms and detectability of aneurysms decreases with heterogeneity in the flow.
Terasaki et al. [42]	Global thresholding	Classification	3D and 2D SE-ResNet	2D MIP and 3D vessel patches	Binary cross entropy	Difficult to optimize 3D CNN without overfitting. Under detection of small aneurysm due to insufficient training samples.
Joo et al. [43]	Two stage vessel segmentation	Classification	3D ResNet	3D vessel patches	Binary cross entropy	Under detection of small aneurysms and specificity was low for vessels with irregular shape.
Stember et al. [49]	-	Segmentation	2D U-net	2D MIP aneurysm patches and its masks	Negative Dice coefficient	False positive rate is high for bifurcation due to MIP representation.
Sichtermann et al. [50]	-	Segmentation	DeepMedic CNN	3D aneurysm patches and its masks	Binary cross entropy	Poor specificity due to the limited number of training samples.
Claux et al. [53]	-	Segmentation	Artery segmentation U-net and modified U-net for aneurysm segmentation	3D aneurysm patches and its masks	Soft dice	Sensitivity was affected by insufficient samples of small and large aneurysms.
Di Noto et al. [54]	-	Segmentation	3D U-net	3D aneurysm patches and its masks	Dice and Crossentropy	Sensitivity of small aneurysm is low due to insufficient samples.

the dataset. Among subjects with unruptured intracranial aneurysms (UIAs) (N = 93), the median age was 55 years (ranging from 24 to 75 years), with 75% of them being female. A subset of the dataset (N = 35) included two scans from each subject: a baseline and a follow-up scan after more than six months. The sizes of the UIAs varied, with a median maximum diameter of 3.6 mm, ranging from 1.0 mm to 15.9 mm. Comparatively, the median age of individuals without UIAs was 41 years (ranging from 19 to 61 years), with 65% being female. All images were pre-processed with N4 bias-field correction [57]. The ADAM training set comprises original and pre-processed data, with this study specifically utilizing the pre-processed data for conducting experiments.

2) LAUSANNE Dataset

The LAUSANNE dataset [54] is an open-access dataset available on OpenNeuro under the CC0 license at https://openneuro.org/datasets/ds003949 and comprises 284 TOF-MRA subjects. Among these, 127 are healthy controls, and 157 are patients with one or more cerebral aneurysms, with 178 saccular and 20 fusiform type aneurysms. Among subjects with unruptured intracranial aneurysms (UIAs) (N = 157), the median age was 56 years, with 66% of them being female. The sizes of the UIAs varied, with a median maximum diameter of 3.7 mm, ranging from 1.0 mm to 20 mm. The median age of individuals without UIAs was 46, with 52% female.

B. EXPERIMENTAL SETUP

This section describes the experimental setup for the comparative analysis, covering input patch selection, training details, model configurations, and evaluation metrics to ensure the reproducibility of the results.

1) Input Patch Selection

A patch sampling technique was utilized to ensure a balanced representation of both positive and negative samples. Using a region-growing-based method, $64\times64\times64$ arterial vessel

patches were extracted, classified as "positive" if they contained aneurysm voxels and "negative" otherwise. Notably, the number of positive patches was lower than that of negative patches. To address this imbalance, Albumentations [58], an open-source library for data augmentation, was employed to generate additional positive samples. Meanwhile, negative samples were randomly downsampled to balance the dataset alongside the positive cases.

2) Training Details

To ensure consistent evaluation across all deep learning models in this study, we established a unified training configuration as follows: all models were trained for 100 epochs with a batch size of 8, utilizing an adaptive learning rate strategy (initial learning rate = 0.001) and the Adam optimizer [59]. Training and evaluation were conducted using PyTorch 2.1.2 + CUDA 12.1 on an NVIDIA A30 Tensor Core GPU with 25 GB of RAM.

3) Model Configurations

Most of the related works in aneurysm detection rely on in-house datasets for model development, which limits the comparability of results. To address this, a comparative analysis of different models requires evaluating their performance on common datasets. Instead of depending on the results presented in the original papers, we trained the state-of-the-art (SOTA) models [39], [40], [42], [43] using the ADAM and LAUSANNE datasets. Our performance analysis is based on these new results.

In this study, pretrained models including VGG16 [64], ResNet18, ResNet34, ResNet50, ResNet101, ResNet152 [45], and DenseNet121 [65] from the PyTorch package were employed to evaluate the performance of popular deep neural network (DNN) models in aneurysm detection.

4) Evaluation metrics

The prediction's sensitivity and false positive rate decide the classification models' reliability, and the evaluation metrics [60]–[62] help to generalize the model's predictive power. In this study, evaluation metrics like accuracy, error rate, true positive rate (sensitivity or recall or TPR), true negative rate (specificity or TNR), false positive rate (FPR), false negative rate (FNR), precision, F1-score, Matthew's correlation coefficient (MCC) [63] and area under the receiver operating characteristics (AUROC or AUC) are used for the analysis. Five-fold cross-validation is employed to compare the model's performance.

C. DISCUSSION

The review considered the existing classification models such as [39], [40], [42], and [43] for the quantitative analysis, and the results are detailed in Table 4. Among these models, the first two are based on 2D CNN, while the model in [43] operates on a 3D CNN framework, and [42] utilizes both 2D and 3D approaches. The study also analysed the performance of popular DNN architecture such as VGG16 [64],

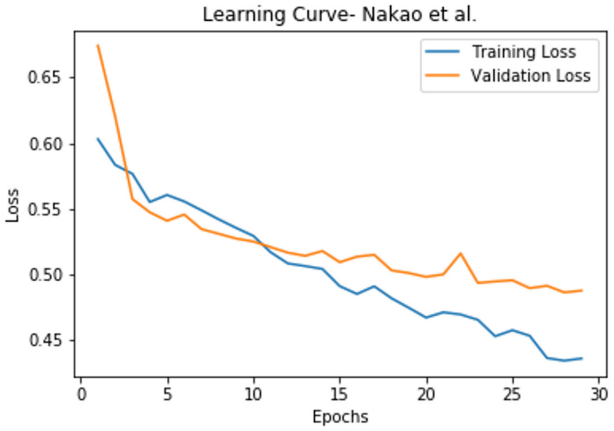

FIGURE 2. **Learning trajectory of shallow model (Nakao et al. [39]) for assessing the impact of overfitting.**

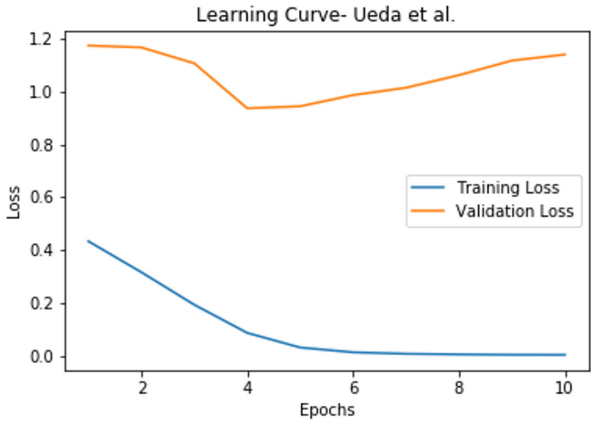

FIGURE 3. **Learning trajectory of complex model (Ueda et al. [40]) for assessing the impact of overfitting.**

ResNet18, ResNet34, ResNet50, ResNet101, ResNet152 [45] and DenseNet121 [65] in the aneurysm classification task, and the analysis is given in the Table 5. The observations are discussed in the following section.

1) Necessity of sufficient data samples

Complex DNN models demand large amounts of data to prevent overfitting. Although complex models perform well in training samples, they often encounter challenges in generalizing to new or unseen data, resulting in overfitting. Table.4 indicates that complex models such as Ueda et al. [40] and Terasaki et al. [42] struggle to generalize when provided with limited data, ultimately leading to overfitting and yielding lower performance than other models such as Nakao et al. [39] and Joo et al. [43]. The learning curves given in Fig. 2 and Fig. 3 illustrate that complex models like Ueda et al. [40] tend to experience overfitting when trained on a restricted dataset (ADAM). Conversely, simple models such as Nakao et al. [39] show no signs of overfitting during training and

TABLE 4. Performance analysis of existing CAD models in Cerebral Aneurysm Detection using five-fold cross-validation on ADAM and LAUSANNE Datasets

Dataset	Model	Accuracy	Error Rate	TNR	FNR	Precision	F1-Score	AUROC	MCC
ADAM	Nakao et al. [39]	0.70±0.05	0.30±0.05	0.85±0.02	0.50±0.07	0.77±0.03	0.63±0.06	0.71±0.08	0.41±0.08
	Ueda et al. [40]	0.64±0.08	0.36±0.08	0.89±0.08	0.63±0.23	0.60±0.34	0.45±0.26	0.69±0.11	0.28±0.16
	Terasaki et al. [42]	0.59±0.06	0.41±0.06	0.48±0.42	0.30±0.38	0.65±0.18	0.56±0.22	0.59±0.07	0.23±0.14
	Joo et al. [43]	0.77±0.04	0.23±0.04	0.87±0.04	0.34±0.08	0.82±0.03	0.73±0.04	0.86±0.04	0.54±0.08
LAUSANNE	Nakao et al. [39]	0.74±0.06	0.26±0.06	0.75±0.07	0.37±0.06	0.21±0.04	0.31±0.04	0.75±0.03	0.25±0.04
	Ueda et al. [40]	0.70±0.03	0.30±0.03	0.69±0.03	0.27±0.06	0.19±0.01	0.30±0.02	0.77±0.02	0.25±0.02
	Terasaki et al. [42]	0.70±0.29	0.30±0.29	0.74±0.36	0.75±0.39	0.05±0.04	0.07±0.08	0.59±0.14	0.05±0.03
	Joo et al. [43]	0.75±0.10	0.25±0.10	0.76±0.12	0.34±0.17	0.23±0.05	0.33±0.03	0.79±0.02	0.28±0.02

TABLE 5. Performance analysis of popular DNN models with three different variants: Model A: Architectures initialized with random weights, Model B: architectures initialized with weights pre-trained on ImageNet, and Model C: architectures with pre-trainable parameters set to false.

Model	Model Type	Accuracy	Error Rate	TNR	FNR	Precision	F1-Score	AUROC	MCC
ResNet18 [45]	Model A	0.64±0.08	0.36±0.08	0.89±0.08	0.63±0.23	0.60±0.34	0.45±0.26	0.69±0.11	0.28±0.16
	Model B	0.78±0.04	0.22±0.04	0.89±0.03	0.33±0.07	0.85±0.03	0.75±0.05	0.86±0.03	0.58±0.08
	Model C	0.72±0.02	0.28±0.02	0.86±0.02	0.44±0.06	0.78±0.04	0.65±0.04	0.79±0.03	0.44±0.04
ResNet34 [45]	Model A	0.56±0.09	0.44±0.09	0.97±0.08	0.88±0.26	0.16±0.34	0.30±0.13	0.53±0.17	0.09±0.19
	Model B	0.77±0.04	0.23±0.04	0.84±0.04	0.30±0.07	0.80±0.04	0.74±0.04	0.85±0.03	0.54±0.07
	Model C	0.70±0.03	0.30±0.03	0.84±0.04	0.43±0.07	0.76±0.04	0.64±0.04	0.79±0.02	0.41±0.05
ResNet50 [45]	Model A	0.59±0.07	0.41±0.07	0.89±0.11	0.73±0.26	0.42±0.38	0.32±0.30	0.63±0.08	0.17±0.16
	Model B	0.76±0.04	0.24±0.04	0.86±0.03	0.35±0.05	0.81±0.03	0.72±0.04	0.83±0.04	0.52±0.06
	Model C	0.64±0.02	0.36±0.02	0.90±0.02	0.64±0.03	0.77±0.06	0.49±0.04	0.74±0.01	0.31±0.05
ResNet101 [45]	Model A	0.62±0.03	0.38±0.03	0.86±0.05	0.64±0.09	0.70±0.07	0.47±0.08	0.69±0.04	0.25±0.07
	Model B	0.74±0.04	0.26±0.04	0.85±0.02	0.38±0.08	0.79±0.04	0.69±0.06	0.82±0.03	0.49±0.07
	Model C	0.62±0.04	0.38±0.04	0.88±0.02	0.65±0.07	0.73±0.03	0.47±0.06	0.73±0.02	0.80±0.04
ResNet152 [45]	Model A	0.60±0.07	0.40±0.07	0.83±0.12	0.65±0.24	0.52±0.30	0.41±0.25	0.66±0.10	0.20±0.14
	Model B	0.76±0.05	0.24±0.05	0.86±0.03	0.36±0.08	0.81±0.03	0.72±0.07	0.82±0.05	0.53±0.09
	Model C	0.68±0.06	0.32±0.06	0.89±0.01	0.54±0.12	0.79±0.03	0.58±0.09	0.77±0.05	0.39±0.09
VGG16 [64]	Model A	0.72±0.05	0.28±0.05	0.83±0.04	0.40±0.07	0.77±0.04	0.67±0.06	0.79±0.07	0.44±0.09
	Model B	0.79±0.01	0.21±0.01	0.89±0.02	0.31±0.02	0.85±0.02	0.76±0.01	0.89±0.01	0.59±0.02
	Model C	0.67±0.04	0.33±0.04	0.90±0.02	0.57±0.07	0.79±0.04	0.55±0.05	0.77±0.04	0.37±0.06
DenseNet [65]	Model A	0.72±0.06	0.28±0.06	0.83±0.03	0.39±0.12	0.77±0.02	0.67±0.09	0.81±0.05	0.45±0.10
	Model B	0.78±0.05	0.22±0.05	0.86±0.02	0.30±0.09	0.82±0.03	0.75±0.06	0.87±0.04	0.57±0.08
	Model C	0.72±0.03	0.28±0.03	0.85±0.04	0.42±0.05	0.79±0.05	0.66±0.03	0.80±0.03	0.45±0.05

demonstrate improved performance on unfamiliar data.

2) Trade-off between Sensitivity and False Positive Rate

A reliable CAD system must show high sensitivity towards aneurysm samples with fewer false alarms. Fig. 4 shows that deeper CNN models such as Terasaki et al. [42] and Ueda et al. [40] fail to maintain the trade-off between sensitivity and FPR compared to shallower CNN architectures of Nakao et al. [39] and Joo et al. [43]. Even though the sensitivity of [42] reaches 70%, they tend to produce over 50% false positives.

3) Suitable representation of MRI-TOF data

Another factor affecting the CAD system's performance is the type of samples fed into the network. MIP representation may lead to under-detection due to various factors, such as the unusual locations of aneurysms and overlapping of aneurysms with the blood vessels [12], [39] and the quality of MIP images. MIP representation is susceptible to the noises present in the MRA TOF sequence.

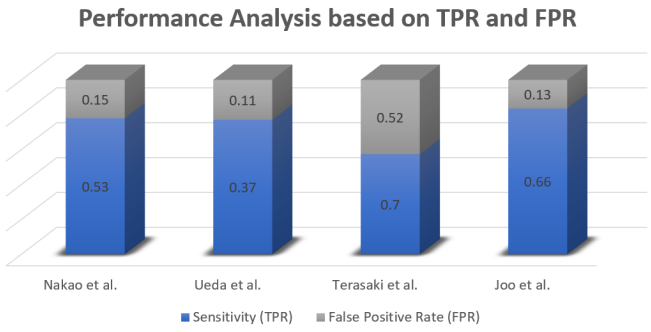

FIGURE 4. **Performance of state-of-the-art models based on Sensitivity and False Positives**

4) Two-dimensional Vs Three-dimensional Convolutional Neural Networks

The inter-dependency among the MRI slices helps to identify the aneurysm in the vascular structure. 3D CNN architectures considered this long-term dependency for decision-making. Conversely, 2D CNN captures only spatial information and does not consider this topological information. From the FROC analysis given in Fig. 5, it is evident that the 3D architecture of Joo et al. [43] surpasses the 2D architectures of Nakao et al. [39] and Ueda et al. [40] in the classification task. Hence, 3D CNN models are more suitable for detecting cerebral aneurysms from TOF MRI sequences compared to 2D models.

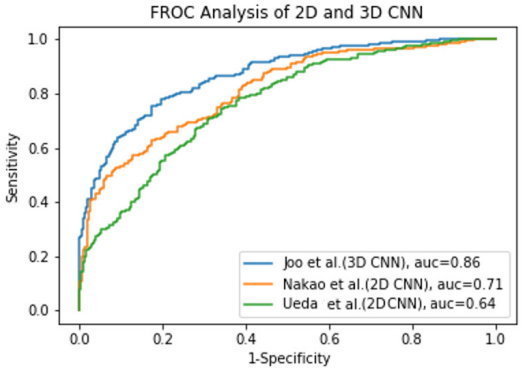

FIGURE 5. **FROC analysis of 2D and 3D CNN architectures**

5) Impact of deepness on network architecture

The review performs a comparative study of ResNet architecture across various depths to study the influence of deepness, selecting ResNet18, ResNet50 and ResNet101 architectures initialized with weights pre-trained on ImageNet for evaluation. As indicated in Fig. 6 , it is evident that ResNet18 outperforms the other networks. The study observes that shallower CNN models exhibit greater suitability for aneurysm detection tasks than deeper architectures.

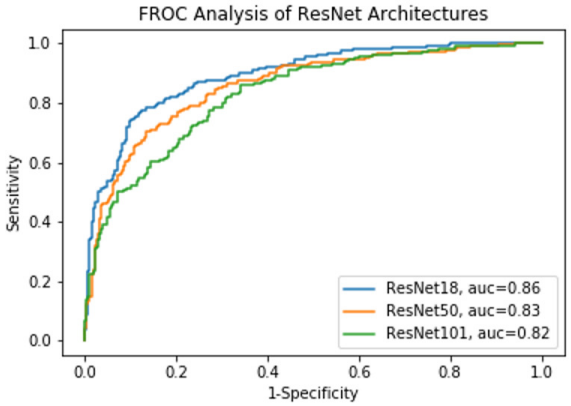

FIGURE 6. **FROC analysis of different ResNet Architectures**

6) Effectiveness of Transfer Learning

Transfer learning approaches have been widely used in the medical domain to overcome data scarcity and computational requirements [66], [67]. To investigate the impact of transfer learning, three different variants of model initialization were tested:

a) **Model A** (Random Initialization): Architectures initialized with random weights, allowing the models to learn from scratch based on the training data.
b) **Model B** (Pretrained on ImageNet): Architectures initialized with weights pre-trained on ImageNet, enabling the models to utilize learned features from a large-scale natural image dataset for improved generalization.
c) **Model C** (Frozen Pre-trained Parameters): Architectures with pre-trainable parameters set to false, effectively freezing the pre-trained weights to retain their learned features without further adaptation during training.

These configurations were designed to explore the effectiveness of transfer learning in enhancing the performance of DNN models for aneurysm detection. Table 5 and Fig. 7 indicate that the pretrained model with ImageNet weight performs well with the ADAM data set. Therefore, transfer learning is an effective solution for converging a complex model with limited training samples like the ADAM dataset.

IV. CAD FOR CEREBRAL ANEURYSM DETECTION: A FUTURE PERSPECTIVE

This section provides an overview of the key considerations in developing a CAD system for aneurysm detection. Recent CAD system advancements help the clinicians to reduce their workload and turn-around time in the clinical environment. However, the current computing approaches have limitations in fully utilizing the information embedded in the TOF MRA data. The review highlights these challenges and provides suggestions for addressing them.

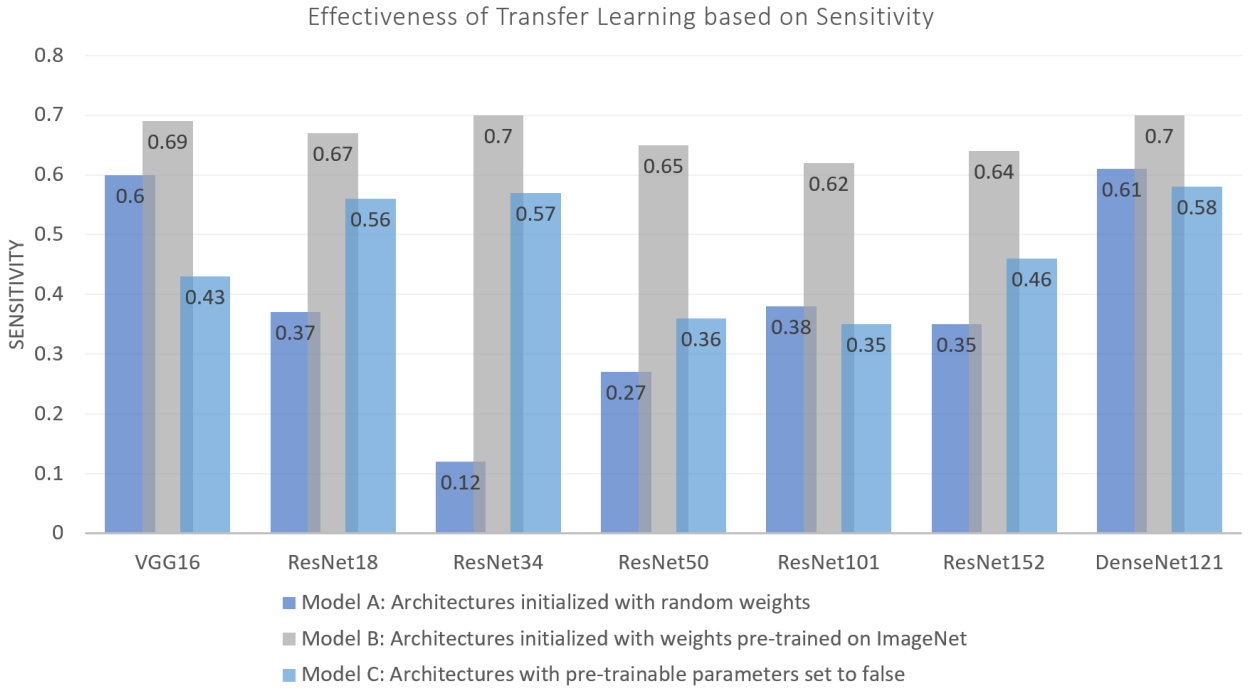

FIGURE 7. **Effectiveness of Transfer Learning in Detecting Cerebral Aneurysms Using the ADAM Dataset**

1) Data Availability and Imbalance in Aneurysm Detection

Cerebral aneurysm detection problems are often constrained by data availability and unbalanced data distribution. Several data augmentation techniques are available in the literature [68], [69] to handle the data availability and unbalanced problem. Conventional data augmentation techniques rely upon linear and label-preserving transformation-based algorithms. Recent studies show that evolutionary learning-based and generative adversarial networks (GAN) based non-linear transformation techniques [70]–[72] are better suited for handling medical data augmentation problems than linear techniques.

Self-Supervised Learning (SSL) [73] is an effective approach for training models with limited labeled data. It utilizes unlabeled data to enable the network to learn meaningful representations without needing labeled examples. When integrated with GAN, SSL can generate additional synthetic data samples, making it a powerful augmentation technique for addressing imbalanced data distribution in medical domain challenges, such as aneurysm detection.

2) Capturing Long-Range Dependencies in Aneurysm Detection

The capability of capturing haemodynamic flow make the TOF MRA sequence the most widely accepted tool for detecting unruptured aneurysms. Hence to fully capture these characteristics, the model must utilise the long-range dependencies. CNN achieved this by deeply stacked convolutional layers but with high computational complexity. Alternatively, attention models, inspired by the transformer architecture [74] serve the same purpose, yet these techniques often require excessive memory usage, leading to inefficient and unnecessarily complex architectures. Graph neural networks (GNN) [75] have emerged as a powerful tool for capturing long-term dependencies, offering researchers a valuable method for aneurysm detection.

V. CONCLUSION

This article provides a detailed review of the development of CAD models for aneurysm detection using TOF-MRA volume. The review systematically analyses the different CAD systems available in the literature and highlights key challenges in developing CAD system for aneurysm detection.

One of the main challenges is the availability of sufficient balanced data samples essential for training deep learning models without overfitting. Another challenge identified is the limitation of CNN models in effectively capturing long-range dependencies within the 3D TOF-MRA volume, which are crucial for identifying key features in the vessel structure for aneurysm detection. The review highlights the significance of low-level features in aneurysm detection, indicating that shallow networks outperform deeper networks in this task, mainly when dealing with limited samples and avoiding overfitting.

The review suggests that transfer learning, self-supervised learning, and GAN-based models are promising candidates for addressing the data scarcity challenges in developing CAD systems for aneurysm detection. GNN and attention-

based models can be effectively adopted for CAD development to capture the long-range dependencies in the 3D TOF-MRA volume to enhance the detection performance. These approaches can capture the unique characteristics of 3D TOF-MRA volume more effectively, advancing the field of cerebral aneurysm detection.

ACKNOWLEDGMENT

The first author is thankful to the University Grants Commission (UGC) of India for financial support through UGC-JRF fellowship-NTA Ref.No. 210510076010.

We also, acknowledge the support received from the computing facility at the Department of Computer Science, Cochin University of Science and Technology (CUSAT), sponsored by Kerala State Higher Education Council (KSHEC) under the Kairali Research Award 2020 Project (File No: KSHEC-A3/352/Kairali Research Award/47/2022).

REFERENCES

[1] Jonathan L Brisman, Joon K Song, and David W Newell, ''Cerebral aneurysms,'' *The New England journal of medicine*., vol. 355, no. 9, pp. 928-939,2006. DOI:10.1056/NEJMra052760.

[2] T Ingall, K Asplund, M Mahonen, and RBonita, "A multinational comparison of sub arachnoid hemorrhage epidemiology in the WHO MONICA stroke study," *Stroke*., vol. 31, no. 5, pp. 1054–1061, 2000. DOI: 10.1161/01.str.31.5.1054.

[3] The International Study of Unruptured Intracranial Aneurysms Investigators, " Unruptured intracranial aneurysms—Risk of rupture and risks of surgical intervention," *The New England Journal of Medicine*., vol. 339, pp. 1725-1733, Dec. 1998. DOI: 10.1056/NEJM199812103392401.

[4] Nefize Turan, Robert A. Heider, Anil K. Roy, Brandon A. Miller, Mark E. Mullins, Daniel L. Barrow, Jonathan Grossberg, and Gustavo Pradilla," Current Perspectives in Imaging Modalities for the Assessment of Unruptured Intracranial Aneurysms: A Comparative Analysis and Review," *World Neurosurgery*, vol. 113, pp. 280–292, 2018. DOI: 10.1016/j.wneu.2018.01. 054.

[5] Nam K. Yoon, Scott McNally, Philipp Taussky, and Min S. Park," Imaging of cere bral aneurysms: a clinical perspective," *Neurovascular Imaging*, vol. 2, no. 6, 2016. DOI: 10.1186/s40809-016-0016-3.

[6] Malikeh Nabaei, "Cerebral aneurysm evolution modeling from microstructural computational models to machine learning: A review," *Computational Biology and Chemistry*, vol. 98, pp. 107676, 2022. DOI: 10.1016/j.compbiolchem.2022.107676.

[7] Din M, Agarwal S, Grzeda M, et al., "Detection of cerebral aneurysms using artificial intelligence: a systematic review and meta-analysis," *Journal of NeuroInterventional Surgery*, vol. 1265, pp. 262-271, 2023.

[8] S. Nafees Ahmed and P. Prakasam, "A systematic review on intracranial aneurysm and hemorrhage detection using machine learning and deep learning techniques," *Progress in Biophysics and Molecular Biology*, vol. 183, pp.1–16, 2023. DOI: 10.1016/j.pbiomolbio.2023.07.001.

[9] Hidetaka Arimura, Qiang Li, Yukunori Korogi, Toshinori Hirai, Hiroyuki Abe, Yasuyuki Yamashita, Shigehiko Katsura gawa, Ryuji Ikeda, and Kunio Doi, "Automated computerized scheme for detection of unruptured intracranial aneurysms in three dimensional magnetic resonance angiography," *Academic Radiology*, vol. 11, no. 10, pp. 1093–1104, 2004. DOI: 10.1016/j.acra.2004.07.011.

[10] Y. Uchiyama, H. Ando, R. Yokoyama, T. Hara, H. Fujita, and T. Iwama, "Computer Aided Diagnosis Scheme for Detection of Unruptured Intracranial Aneurysms in MR Angiography," *in 2005 IEEE Engineering in Medicine and Biology 27th Annual Conference*, 2005, pp. 3031–3034, 2005. DOI: 10.1109/IEMBS.2005.1617113.

[11] Hidetaka Arimura, Qiang Li, Yukunori Korogi, Toshinori Hirai, Hiroyuki Abe, Yasuyuki Yamashita, Shigehiko Katsura gawa, Ryuji Ikeda, and Kunio Doi, "Development of CADschemeforautomated detection of intracranial aneurysms in magnetic resonance angiography," *International Congress Series*, vol. 1268, pp. 1015–1020, 2004. DOI: 10.1016/j.ics.2004.03.102.

[12] Syoji Kobashi, Katsuya Kondo, and Yutaka Hata, "Computer-Aided Diagnosis of Intracranial Aneurysms in MRA Images with Case Based Reasoning," *IEICE Transactions*, vol. 89-D, pp. 340–350, 2006. DOI: 10.1093/ietisy/e89-d.1.340.

[13] Syoji Kobashi, Naotake Kamiura, Yutaka Hata, and Fujio Miyawaki, "Fuzzy Information Granulation on Blood Vessel Extraction from 3D TOF MRAImage," *IJPRAI*, vol. 14, pp. 409-425,2000. DOI: 10.1142/S0218001400000271.

[14] S Kobashi, N Kamiura, Y Hata, and FMiyawaki, "Volume-quantization-based neural network approach to 3D MR angiography image segmentation," *Image and Vision Computing*, vol. 1, no. 4, pp. 185–193, 2001. DOI: 10.1016/S0262-8856(00)00067-6.

[15] Xiaojiang Yang, Daniel J. Blezek, Lionel T. E. Cheng, William J. Ryan, David F. Kallmes, and Bradley J. Erickson, "Computer Aided Detection of Intracranial Aneurysms in MR Angiography," *J Digit Imaging*, vol. 24, pp. 86–95, 2011. DOI: 10.1007/s10278-009-9254-0.

[16] Santiago Suniaga, Rene Werner, Andre Kemmling, Michael Groth, Jens Fiehler, and Nils Daniel Forkert, "Computer-Aided Detection of Aneurysms in 3D Time-of-Flight MRA Datasets," *Machine Learning in Medical Imaging*, pp. 63–69, 2012.

[17] Nils Daniel Forkert, Dennis S¨aring, Till Illies, Jens Fiehler, Jan Ehrhardt, Heinz Handels, and Alexander Schmidt-Richberg, "Direction dependent Level Set Segmentation of cerebrovascular Structures," *Progress in Biomedical Optics and Imaging- Proceedings of SPIE*, vol. 7962, pp. 351–358, 2011. DOI: 10.1117/12.877942.

[18] Yoshinobu Sato, Shin Nakajima, Nobuyuki Shiraga, Hideki Atsumi, Shigeyuki Yoshida, Thomas Koller, Guido Gerig, and Ron Kikinis, "Three-dimensional multi-scale line filter for segmentation and visualization of curvilinear structures in medical images," *Medical Image Analysis*, vol. 2, no. 2, pp. 143–168, 1998. DOI: 10.1016/S1361-8415(98)80009-1.

[19] Shouhei Hanaoka, Yukihiro Nomura, Mitsutaka Nemoto, Soichiro Miki, Takeharu Yoshikawa, Naoto Hayashi, Kuni Ohtomo, Yoshitaka Masutani, and Akinobu Shimizu, "HoTPiG: A Novel Geometrical Feature for Vessel Morphometry and Its Application to Cerebral Aneurysm Detection," paper presented at *Medical Image Computing and Computer-Assisted Intervention– MICCAI 2015*, pp. 103–110, 2015.

[20] Yukihiro Nomura, Yoshitaka Masutani, Soichiro Miki, Mitsutaka Nemoto, Shouhei Hanaoka, Takeharu Yoshikawa, Naoto Hayashi, and Kuni Ohtomo, "Performance improvement in computerized detection of cerebral aneurysms by retraining classifier using feedback data collected in routine reading environment," *Journal of Biomedical Graphics and Computing*, vol. 4, 2014. DOI: 10.5430/jbgc.v4n4p12.

[21] Hidetaka Arimura, Qiang Li, Yukunori Korogi, Toshinori Hirai, Shigehiko Kat suragawa, Yasuyuki Yamashita, Kazuhiro Tsuchiya, and Kunio Doi, "Computerized detection of intracranial aneurysms for three-dimensional MR angiography: Feature extraction of small protrusions based on a shape-based difference image technique," *Medical physics*, vol. 33, pp. 394–401, 2006. DOI: 10.1118/1.2163389

[22] Clemens Hentschke, Oliver Beuing, RosaNickl, and Klaus T¨onnies, "Automatic cere bral aneurysm detection in multimodal angiographic images," *IEEE Nuclear Science Symposium Conference Record*, pp. 3116-3120, 2011. DOI: 10.1109/NSSMIC.2011.6152566.

[23] Qiang Li, Shusuke Sone, and Kunio Doi, "Selective enhancement filters for nodules, vessels, and airway walls in two- and three dimensional CT scans," *Medical physics*, vol. 30, pp. 2040–2051, 2003. DOI: 10.1118/1.1581411.

[24] Mitsutaka Nemoto, Akinobu Shimizu, Yoshihiro Hagihara, Hidefumi Kobatake, and Shigeru Nawano, "Improvement of tumor detection performance in mammograms by feature selection from a large number of features and proposal of fast feature selection method," *Systems and Computers in Japan*, vol. 37, no. 12, pp. 56–68, 2006. DOI: 10.1002/scj.20498.

[25] Alejandro F. Frangi, Wiro J. Niessen, Koen L. Vincken, and Max A. Viergever, "Multiscale vessel enhancement filtering," paper presented at *Medical Image Computing and Computer-Assisted Intervention —MICCAI'98*, 1998, pp. 130–137.

[26] H. Kobatake and M. Murakami, "Adaptive filter to detect rounded convex regions: iris filter, " *in Proceedings of 13th International Conference on Pattern Recognition*, vol. 2, pp. 340–344, 1996. DOI: 10.1109/ICPR.1996.546846.

[27] Toyofumi Saito and Jun ichiro Toriwaki, "Reverse Distance Transformation and Skeletons based upon the Euclidean Metric for n-Dimensional Digital Binary Pictures," *IEICE Transactions on Information and Systems*, vol. 77, no. 9, pp. 1005–1016, 1994.

[28] Gunilla Borgefors, Ingela Nystr¨om, and Gabriella Sanniti Di Baja, "Com-

puting skeletons in three dimensions," *Pattern Recognition*, vol. 32, no. 7, pp. 1225–1236, 1999. DOI: 10.1016/S0031-3203(98)00082-X

[29] T. Saito, "A sequential thinning algorithm for three dimensional digital pictures using the euclidean distance transformation, 1995. Available: https://api.semanticscholar.org/CorpusID:124966992.

[30] Toyofumi Saito and Jun-Ichiro Toriwaki, "New algorithms for euclidean distance transformation of an n-dimensional digitized picture with applications," *Pattern Recognition*, vol. 27, no. 11, pp. 1551–1565, 1994. DOI: 10.1016/0031-3203(94)90133-3

[31] T.C. Lee, R.L. Kashyap, and C.N. Chu, "Building Skeleton Models via 3-D Medial Surface Axis Thinning Algorithms," *CVGIP: Graphical Models and Image Processing*, vol. 56, no. 6, pp. 462–478, 1994. DOI: 10.1006/cgip.1994.1042.

[32] Y. Zhou and A.W. Toga, "Efficient skeletonization of volumetric objects," *IEEE Transactions on Visualization and Computer Graphics*, vol. 5, no. 3, pp. 196–209, 1999. DOI: 10.1109/2945.795212.

[33] M.A. Forstner and E Gulch, "A Fast Operator for Detection and Precise Location of Distinct Points, Corners and Centers of Circular Features," *in Proceedings of the ISPRS Intercommission Conference on Fast Processing of Phonogrammic Data*, 1987, pp. 281–305.

[34] J. Kolodner, "Case-based reasoning," San Mateo, CA: Morgan Kaufmann Publishers, 1993.

[35] Thorsten Joachims, "Making large scale SVM learning practical," *Advances in Kernel Methods: Support Vector Machines*, vol. 10, 1999. DOI: 10.17877/DE290R-5098.

[36] Peter Bartlett, Yoav Freund, Wee Sun Lee, and Robert E. Schapire, "Boosting the margin: a new explanation for the effectiveness of voting methods," *The Annals of Statistics*, vol. 26, no. 5, pp. 1651– 1686, 1998. DOI: 10.1214/aos/1024691352.

[37] S. Miki, N. Hayashi, Y. Masutani, Y. Nomura, T. Yoshikawa, S. Hanaoka, M. Nemoto, and K. Ohtomo, "Computer Assisted Detection of Cerebral Aneurysms in MR Angiography in a Routine Image Reading Environment: Effects on Diagnosis by Radiologists," *American Journal of Neuro Radiology*, vol. 37, np. 6, pp. 1038–1043, 2016. DOI: 10.3174/ajnr.A4671.

[38] Yann LeCun, Y. Bengio, and Geoffrey Hinton, "Deep learning," *Nature*, vol. 521, pp. 436-444, 2015. DOI: 10.1038/nature14539.

[39] Takahiro Nakao, Shouhei Hanaoka, Yukihiro Nomura, Issei Sato, Mitsutaka Nemoto, Soichiro Miki, Eriko Maeda, Takeharu Yoshikawa, Naoto Hayashi, and Osamu Abe, "Deep neural network-based computer assisted detection of cerebral aneurysms in MR angiography," *Journal of Magnetic Resonance Imaging*, vol. 47, no. 4, pp. 948–953, 2018. DOI: 10.1002/jmri.25842.

[40] Daiju Ueda, Akira Yamamoto, Masataka Nishimori, Taro Shimono, Satoshi Doishita, Akitoshi Shimazaki, Yutaka Katayama, Shinya Fukumoto, Antoine Choppin, Yuki Shimahara, and Yukio Miki, "Deep Learning for MR Angiography: Automated Detection of Cerebral Aneurysms," *Radiology*, vol. 290, no. 1, pp. 187–194, 2019. DOI: 10.1148/radiol.2018180901.

[41] Naoto Hayashi, Yoshitaka Masutani, Tomohiko Masumoto, Harushi Mori, Akira Kunimatsu, Osamu Abe, Shigeki Aoki, Kuni Ohtomo, Naoki Takano, and Kazuhiko Matsumoto, "Feasibility of a Curvature-based Enhanced Display System for Detecting Cerebral Aneurysms in MR Angiography," *Magnetic Resonance in Medical Sciences*, vol. 2, no. 1, pp. 29–36, 2003. DOI: 10.2463/mrms.2.29

[42] Yuki Terasaki, Hajime Yokota, Kohei Tashiro, Takuma Maejima, Takashi Takeuchi, Ryuna Kurosawa, Shoma Yamauchi, Akiyo Takada, Hiroki Mukai, Kenji Ohira, Joji Ota, Takuro Horikoshi, Yasukuni Mori, Takashi Uno, and Hiroki Suyari, "Multidimensional Deep Learning Reduces False-Positives in the Automated Detection of Cerebral Aneurysms on Time-Of-Flight Magnetic Resonance Angiography: A Multi-Center Study," *Frontiers in Neurology*, vol. 12, 2022. DOI: 10.3389/fneur.2021.742126.

[43] Bio Joo, Sung Ahn, Pyeong Yoon, Sohi Bae, Beomseok Sohn, Yong Lee, Jun Bae, Moo Park, Hyun Choi, and Seung-Koo Lee, "A deep learning algorithm may automate intracranial aneurysm detection on MR angiography with high diagnostic performance," *European Radiology*, vol. 30, 2020. DOI: 10.1007/ s00330-020-06966-8.

[44] Rui Wang, Chao Li, Jie Wang, Xiaoer Wei, Yuehua Li, Yuemin Zhu, and Su Zhang, "Threshold segmentation algorithm for automatic extraction of cerebral vessels from brain magnetic resonance angiography images," *Journal of Neuroscience Methods*, vol. 241, pp. 30–36, 2015. DOI: 10.1016/j.jneumeth.2014.12.003.

[45] Kaiming He, Xiangyu Zhang, Shaoqing Ren, and Jian Sun, "Deep Residual Learning for Image Recognition," *in 2016 IEEE Conference on Computer Vision and Pattern Recognition (CVPR)*, 2016, pp. 770–778, 2016. DOI: 10.1109/CVPR.2016.90.

[46] Du Tran, Heng Wang, Lorenzo Torresani, Jamie Ray, Yann LeCun, and Manohar Paluri, "A closer look at spatiotemporal convolutions for action recognition," *in Proceedings of the IEEE/CVF Conference on Computer Vision and Pattern Recognition (CVPR)*, 2018, pp. 6450–6459. DOI: 10.1109/CVPR.2018.00675

[47] Jie Hu, Li Shen, and Gang Sun, "Squeeze-and Excitation Networks," *in Proceedings of the IEEE/CVF Conference on Computer Vision and Pattern Recognition*, 2018, pp. 7132–7141. DOI: 10.1109/CVPR.2018.00745.

[48] Olaf Ronneberger, Philipp Fischer, and Thomas Brox, "U-Net: Convolutional Net works for Biomedical Image Segmentation," *paper presented at Medical Image Computing and Computer-Assisted Intervention– MICCAI 2015*, 2015, pp. 234–241.

[49] Joseph Stember, Peter Chang, Danielle Stember, Michael Liu, Jack Grinband, Christopher Filippi, Philip Meyers, and Sachin Jambawalikar, "Convolutional Neural Networks for the Detection and Measurement of Cerebral Aneurysms on Magnetic Resonance Angiography," *Journal of Digital Imaging*, vol. 32, 2018. DOI: 10.1007/s10278-018-0162-z.

[50] T. Sichtermann, A. Faron, R. Sijben, N. Teichert, J. Freiherr, and M. Wiesmann, "Deep Learning–Based Detection of Intracranial Aneurysms in 3D TOF-MRA," *American Journal of Neuroradiology*, vol. 40, no. 1, pp. 25–32, 2019. DOI: 10.3174/ajnr.A5911.

[51] Konstantinos Kamnitsas, Enzo Ferrante, Sarah Parisot, Christian Ledig, Aditya Nori, Antonio Criminisi, Daniel Rueckert, and Ben Glocker, "DeepMedic for Brain Tumor Segmentation", pp. 138–149, 2016.

[52] Konstantinos Kamnitsas, Christian Ledig, Virginia F.J. Newcombe, Joanna P. Simpson, Andrew D. Kane, David K. Menon, Daniel Rueckert, and Ben Glocker, " Efficient multi scale 3D CNN with fully connected CRF for accurate brain lesion segmentation," *Medical Image Analysis*, vol. 36, pp. 61–78, 2017. DOI: 10.1016/j.media.2016.10.004.

[53] Fr´ed´eric Claux, Maxime Baudouin, Cl´ ement Bogey, and Aymeric Rouchaud, "Dense, deep learning-based intracranial aneurysm detection on TOFMRI using two-stage regularized U-Net," *Journal of Neuroradiology*, vol. 50, no. 1, pp. 9-15, 2023. ISSN 0150-9861. DOI: 10.1016/j.neurad.2022.03.005.

[54] Tommaso Di Noto, Guillaume Marie, S´ebastien Tourbier, Yasser Alem´an-G´omez, Oscar Esteban, Guillaume Saliou, Meritxell Bach Cuadra, Patric Hagmann, and Jonas Richiardi, "Towards Automated Brain Aneurysm Detection in TOF-MRA: Open Data, Weak Labels, and Anatomical Knowledge," *Neuroinformatics*, vol. 21, pp. 1–14, 2022. DOI: 10.1007/s12021-022-09597-0.

[55] Ozgun Cicek, Ahmed Abdulkadir, Soeren S. Lienkamp, Thomas Brox, and Olaf Ronneberger, "3D U-Net: Learning Dense Volumetric Segmentation from Sparse Annotation," *in Proceedings of International Conference on Medical Image Computing and Computer-Assisted Intervention*, 2016.

[56] Kimberley M. Timmins et al., "Comparing methods of detecting and segmenting unruptured intracranial aneurysms on TOF-MRAS: The ADAM challenge," *NeuroImage*, vol. 238, pp. 118216, 2021. DOI: 10.1016/j.neuroimage.2021.118216.

[57] Nicholas J. Tustison, Brian B. Avants, Philip A. Cook, Yuanjie Zheng, Alexander Egan, Paul A. Yushkevich, and James C.Gee, "N4itk: Improved n3 bias correction," *IEEE Transactions on Medical Imaging*, vol. 29, no. 6, pp. 1310–1320, 2010. DOI: 10.1109/TMI.2010.2046908.

[58] Alexander Buslaev, Vladimir Iglovikov, Eugene Khvedchenya, Alex Parinov, Mikhail Druzhinin, and Alexandr Kalinin, "Albumentations: Fast and Flexible Image Augmentations," *Information*, vol. 11, pp. 125, 2020. DOI: 10.3390/info11020125.

[59] Diederik et al., "Adam: A Method for Stochastic Optimization," in *3rd International Conference on Learning Representations, ICLR 2015*, 2015

[60] Mohammad Hossin and Sulaiman M.N, "A Review on Evaluation Metrics for Data Classification Evaluations," *International Journal of Data Mining & Knowledge Management Process*, vol. 5, pp. 01–11, 2015.

[61] Qiong Gu, Li Zhu, and Zhihua Cai, "Evaluation Measures of the Classification Performance of Imbalanced Data Sets," *Computational Intelligence and Intelligent Systems*, pp. 461–471, 2009.

[62] Jin Huang and C.X. Ling, "Using AUC and accuracy in evaluating learning algorithms," *IEEE Transactions on Knowledge and Data Engineering*, vol. 17, no. 3, pp. 299–310, 2005. DOI: 10.1109/TKDE.2005.50.

[63] Davide Chicco and Giuseppe Jurman, "The advantages of the Matthews correlation coefficient (MCC) over F1 score and accuracy in binary classification evaluation," *BMC Genomics*, vol. 21, 2020. DOI: 10.1186/s12864-019-6413-7.

[64] Karen Simonyan and Andrew Zisserman, "Very Deep Convolutional Networks for Large Scale Image Recognition," *in Proceedings of 3rd Inter-*

national Conference on Learning Representations, ICLR 2015, San Diego, CA, USA, May 7-9, 2015.

[65] Gao Huang, Zhuang Liu, Laurens Van Der Maaten, and Kilian Q. Weinberger, "Densely Connected Convolutional Networks," *in Proceedings of IEEE Conference on Computer Vision and Pattern Recognition (CVPR)*, 2017, pp. 2261–2269. DOI: 10.1109/CVPR.2017.243.

[66] Laith Alzubaidi, Ye Duan, Ayad Al-Dujaili, Ibraheem Ibraheem, Ahmed Alkenani, Jose Santamar´ıa, Mohammed Fadhel, Omran Al Shamma, and Jinglan Zhang, "Deepening into the suitability of using pre-trained models of imagenet against a lightweight convolutional neural network in medical imaging: an experimental study," *PeerJ Computer Science*, vol. 09, 2021. DOI: 10.7717/peerj-cs.715.

[67] Srikanth Tammina, "Transfer learning using VGG-16 with Deep Convolutional Neural Network for Classifying Image," *International Journal of Scientific and Research Publications*, vol. 9, no. 10,pp. p9420, 2019. DOI: 10.29322/IJSRP.9.10.2019.p9420.

[68] Dazhi Zhao, Guozhu Yu, Peng Xu, and Maokang Luo, "Equivalence between dropout and data augmentation: A mathematical check," *Neural Networks*, vol. 115, pp. 82–89, 2019. DOI: 10.1016/j.neunet.2019.03.013.

[69] I. Isaev and Sergey Dolenko, "Training with noise as a method to increase noise resilience of neural network solution of inverse problems," *Optical Memory and Neural Networks*, vol. 25, pp. 142–148, 2016. DOI: 10.3103/S1060992X16030085.

[70] Rishi Raj, Jimson Mathew, Santhosh Kumar Kannath, and Jeny Rajan, "Crossover based technique for data augmentation," *Computer Methods and Programs in Biomedicine*, vol. 218, pp. 106716, 2022. DOI: 10.1016/j.cmpb.2022.106716.

[71] Veit Sandfort, Ke Yan, Perry Pickhardt,and Ronald Summers, "Data augmentation using generative adversarial networks (CycleGAN) to improve generalizability in CT segmentation tasks," *Scientific Reports*, vol. 9, 2019. DOI: 10.1038/s41598-019-52737-x.

[72] Harith Al-Sahaf, Ying Bi, Qi Chen, Andrew Lensen, Yi Mei, Yanan Sun, Binh Tran, Bing Xue, and Mengjie Zhang, "A survey on evolutionary machine learning," *Journal- Royal Society of New Zealand*, 2019. DOI: 10.1080/03036758.2019.1609052.

[73] J. Gui et al., "A Survey on Self-Supervised Learning: Algorithms, Applications, and Future Trends," in *IEEE Transactions on Pattern Analysis and Machine Intelligence*, vol. 46, no. 12, pp. 9052-9071, Dec. 2024, DOI: 10.1109/TPAMI.2024.3415112.

[74] Ashish Vaswani, Noam M. Shazeer, Niki Parmar, Jakob Uszkoreit, Llion Jones, Aidan N. Gomez, Lukasz Kaiser, and Illia Polosukhin, "Attention is All you Need," *Neural Information Processing Systems*, 2017.

[75] Jie Zhou, Ganqu Cui, Shengding Hu, Zhengyan Zhang, Cheng Yang, Zhiyuan Liu, Lifeng Wang, Changcheng Li, and Maosong Sun, "Graph neural networks: A review of methods and applications," *AI Open*, vol. 1, pp. 57–81, 2020. DOI: 10.1016/j.aiopen.2021.01.001

KEERTHI A. S. PILLAI received the Bachelors Degree in Technology (B. Tech.) in Computer Science and Engineering from Cochin University of Science and Technology (CUSAT) in the year 2010 and Masters Degree in Technology (M. Tech.) in Computer Science (with specialization in Digital Image Computing) from University of Kerala in the year 2012. She is currently pursuing the Ph.D. in Computer Science (Medical Image Processing) at Cochin University of Science and Technology.

From 2012 to 2019, she was working as Assistant Professor at the Department of Computer Science and Engineering, Sree Buddha College of Engineering, Alappuzha, Kerala, India. Her research interest includes Digital Image Processing, Computer Vision, Medical Image Processing, Soft Computing, and Deep Neural Networks. She was awarded the University Grants Commission (UGC)- Junior Research Fellowship (JRF) of India in 2022.

PREENA K. P. received the Bachelors Degree in Technology (B. Tech.) in Computer Science and Engineering from University of Calicut in the year 1997 and Masters Degree in Technology (M. Tech.) in Software Engineering from Cochin University of Science and Technology (CUSAT) in the year 2010. She is currently pursuing the Ph.D. in Computer Science (Medical Image Processing) at Cochin University of Science and Technology.

She is an experienced teacher with 21 years of teaching expertise, currently working as Assistant Professor at the Department of Computer Science and Engineering, Model Engineering College, Kochi, Kerala, India. Her research interest includes Digital Image Processing, Computer Vision, Medical Image Processing, and Neural Networks.

MADHU S. NAIR is currently working as Professor at the Artificial Intelligence & Computer Vision Lab, Department of Computer Science, Cochin University of Science and Technology (CUSAT). He received his Masters Degree in Computer Applications (M.C.A.) from Mahatma Gandhi University with First Rank in the year 2003, and Masters Degree in Technology (M.Tech.) in Computer Science (with specialization in Digital Image Computing) from University of Kerala with First Rank in the year 2008. He obtained his Ph.D. in Computer Science (Image Processing) from Mahatma Gandhi University in the year 2013. He also holds a Post Graduate Diploma in Client Server Computing (PGDCSC) from Amrita Institute of Computer Technology.

He is a Senior Member of the Institute of Electrical and Electronics Engineers (IEEE), Senior Member of the Association for Computing Machinery (ACM), Associate Life Member of Computer Society of India (CSI), and Member of the International Association of Engineers (IAENG). He has published 117 research papers in reputed International Journals and Conference Proceedings published by IEEE, Springer, Elsevier, Wiley, IOS Press, etc. He is a recipient of prestigious awards such as AICTE Visvesvaraya Best Teacher Award, Kairali Gaveshana Puraskaram of Govt. of Kerala, Swami Vivekananda Yuva Prathibha Puraskaram of Govt. of Kerala, CSI Best Faculty of the Year Award, Best Thesis Supervisor Award from IEEE Communications Society, etc. His research interests include Digital Image Processing, Pattern Recognition, Computer Vision, Data Compression, Soft Computing, and Scientometrics.